Field-dependent quasiparticles in the infinite-dimensional Hubbard model

J. Bauer and A. C. Hewson
Department of Mathematics, Imperial College, London SW7 2AZ, United Kingdom
(Received 12 December 2006; revised manuscript received 25 May 2007; published 25 July 2007)

We present dynamical mean-field theory (DMFT) results for the local spectral densities of the one- and two-particle response functions for the infinite-dimensional Hubbard model in a magnetic field. We look at the different regimes corresponding to half-filling, near half-filling, and well away from half-filling, for intermediate and strong values of the local interaction U. The low energy results are analyzed in terms of quasiparticles with field-dependent parameters. These renormalized parameters are determined by two different methods, both based on numerical renormalization group (NRG) calculations, and we find good agreement. Away from half-filling, the quasiparticle weights, $z_\sigma(H)$, differ according to the spin type $\sigma=\uparrow$ or $\sigma=\downarrow$. Using the renormalized parameters, we show that DMFT-NRG results for the local longitudinal and transverse dynamic spin susceptibilities in an arbitrary field can be understood in terms of repeated scattering of these quasiparticles. We also check Luttinger's theorem for the Hubbard model and find it to be satisfied in all parameter regimes and for all values of the magnetic field.

DOI: 10.1103/PhysRevB.76.035118 PACS number(s): 71.10.Fd, 71.27.+a

I. INTRODUCTION

A feature of strongly correlated electron systems, such as heavy fermions, is their sensitivity to an applied magnetic field, which makes a magnetic field a useful experimental probe of strong correlation behavior. A manifestation of this sensitivity is the very large paramagnetic susceptibility observed in these systems. In terms of Fermi liquid theory, the large paramagnetic susceptibility can be interpreted as due to quasiparticles with exceptionally large effective masses. These large effective masses arise from the scattering of the electrons with the enhanced spin fluctuations induced by the strong local Coulomb interactions. An applied magnetic field suppresses the spin fluctuations causing a reduction in the effective masses, which can be seen experimentally in de Haas–van Alphen measurements.[1,2] Not only do the effective masses depend on the magnetic field, they may also differ for the spin up and spin down electrons.[3,4] Another feature that reflects the enhanced sensitivity to an applied field is the metamagnetic behavior, where the spin susceptibility $\chi(H)$ in a finite field H increases with the field strength such that $d\chi(H)/dH>0$, which has been observed in some heavy fermion compounds.[5] This can be understood in terms of an increase in the effective mass for larger fields opposite to the effect described above. It is related to the fact that strong magnetic fields can induce localization in narrow conduction bands as predicted theoretically.[6–8] This has been observed experimentally, for instance, in quasi-two-dimensional organic conductors.[9]

A lattice model which can mimic many of these effects is the single band Hubbard model. It has played a similar role for lattice models as the Anderson model for impurity models, being the simplest model of its type, where the interplay of kinetic energy and strong local interactions can be studied. Here, we are interested in studying the magnetic response of this model for different interactions and fillings. The calculations are based on the dynamical mean-field theory (DMFT) with the numerical renormalization group (NRG) to solve the effective impurity problem. We present results for the local spectral densities and spin dynamics in parameter regimes at half-filling and for finite hole doping, where different responses to the magnetic field can be observed.

We interpret the low energy results in terms of quasiparticles which are characterized by field-dependent renormalized parameters. The approach is similar to that used earlier[10,11] for the Anderson model in a magnetic field. We deduce the renormalized parameters by two different methods based on the NRG calculations. These parameters can be used to define a free quasiparticle density of states, which gives the asymptotically exact spectral behavior for low energy. The effects of the interactions between these quasiparticles can be taken into account using a renormalized perturbation theory (RPT).[12,13] It was shown earlier that a very good description of the $T=0$ spin and charge dynamics for the Anderson model in the Kondo regime can be obtained by summing the RPT diagrams for repeated quasiparticle scattering.[14] Here, we extend these RPT calculations for the spin dynamics to the lattice case and show that we can also understand the DMFT-NRG for the local dynamic spin susceptibilities in terms of quasiparticle scattering.

II. DYNAMICAL MEAN-FIELD APPROACH AND RENORMALIZED PARAMETERS

The Hamiltonian for the Hubbard model in a magnetic field in the grand canonical formulation is given by

$$H_\mu = \sum_{i,j,\sigma} (t_{ij} c^\dagger_{i,\sigma} c_{j,\sigma} + \text{H.c.}) - \sum_{i\sigma} \mu_\sigma n_{i\sigma} + U \sum_i n_{i,\uparrow} n_{i,\downarrow}, \quad (1)$$

where t_{ij} are the hopping matrix elements between sites i and j, and U is the on-site interaction; $\mu_\sigma=\mu+\sigma h$, where μ is the chemical potential of the interacting system, and the Zeeman splitting term with external magnetic field H is given by $h=g\mu_B H/2$, where μ_B is the Bohr magneton. We are dealing with the one s-band Hubbard model here, so no coupling of the field to angular momentum states has to be included.

From Dyson's equation, the Green's function $G_{k,\sigma}(\omega)$ can be expressed in the form

$$G_{\boldsymbol{k},\sigma}(\omega) = \frac{1}{\omega + \mu_\sigma - \Sigma_\sigma(\boldsymbol{k},\omega) - \varepsilon(\boldsymbol{k})}, \tag{2}$$

where $\Sigma_\sigma(\boldsymbol{k},\omega)$ is the proper self-energy and $\varepsilon(\boldsymbol{k}) = \Sigma_{\boldsymbol{k}} e^{-\boldsymbol{k}\cdot(\boldsymbol{R}_i - \boldsymbol{R}_j)} t_{ij}$. The simplification that occurs for the model in the infinite-dimensional limit is that $\Sigma_\sigma(\boldsymbol{k},\omega)$ becomes a function of ω only.[15,16] In this case, the local Green's function $G^{\mathrm{loc}}_\sigma(\omega)$ can be expressed in the form

$$G^{\mathrm{loc}}_\sigma(\omega) = \sum_{\boldsymbol{k}} G_{\boldsymbol{k},\sigma}(\omega) = \int d\varepsilon \frac{D(\varepsilon)}{\omega + \mu_\sigma - \Sigma_\sigma(\omega) - \varepsilon}, \tag{3}$$

where $D(\varepsilon)$ is the density of states for the noninteracting model ($U=0$). It is possible to convert this lattice problem into an effective impurity problem.[17] We introduce the dynamical Weiss field $\mathcal{G}^{-1}_{0,\sigma}(\omega)$ and write the Green's function in the form

$$G^{\mathrm{loc}}_\sigma(\omega) = \frac{1}{\mathcal{G}^{-1}_{0,\sigma}(\omega) - \Sigma_\sigma(\omega)}, \tag{4}$$

which is equivalent to

$$\mathcal{G}^{-1}_{0,\sigma}(\omega) = G^{\mathrm{loc}}_\sigma(\omega)^{-1} + \Sigma_\sigma(\omega). \tag{5}$$

The Green's function $G^{\mathrm{loc}}_\sigma(\omega)$ can be identified with the Green's function $G_\sigma(\omega)$ of an effective Anderson model by reexpressing $\mathcal{G}^{-1}_{0,\sigma}(\omega)$ as

$$\mathcal{G}^{-1}_{0,\sigma}(\omega) = \omega + \mu + \sigma h - K_\sigma(\omega), \tag{6}$$

so that

$$G_\sigma(\omega) = \frac{1}{\omega - \varepsilon_{d\sigma} - K_\sigma(\omega) - \Sigma_\sigma(\omega)}, \tag{7}$$

with $\varepsilon_{d\sigma} = -\mu_\sigma$. The function $K_\sigma(\omega)$ plays the role of a dynamical mean field describing the effective medium surrounding the impurity. In the impurity case in the wide band limit, we have $K_\sigma(\omega) = -i\Delta$. Here, as can be seen from Eqs. (5) and (4), $K_\sigma(\omega)$ is a function of the self-energy $\Sigma_\sigma(\omega)$ and hence depends on σ. As this self-energy is identified with the impurity self-energy, which will depend on the form taken for $K_\sigma(\omega)$, it is clear that this quantity has to be calculated self-consistently. Starting from an initial form for $K_\sigma(\omega)$, $\Sigma_\sigma(\omega)$ is calculated using an appropriate "impurity solver" from which $G^{\mathrm{loc}}_\sigma(\omega)$ can be calculated using Eq. (3), and a new result for $K_\sigma(\omega)$ from Eqs. (5) and (6). This $K_\sigma(\omega)$ serves as an input for the effective impurity problem and the process is repeated until it converges to give a self-consistent solution. These equations constitute the DMFT, and further details can be found in the review article of Georges *et al.*[17]

We need to specify the density of states $D(\varepsilon)$ of the noninteracting infinite-dimensional model, which is usually taken to be either for a tight-binding hypercubic or Bethe lattice. Here, we take the semielliptical form corresponding to a Bethe lattice,

$$D(\varepsilon) = \frac{2}{\pi D^2}\sqrt{D^2 - (\varepsilon + \mu_0)^2}, \tag{8}$$

where $2D$ is the bandwidth, with $D = 2t$ for the Hubbard model, and μ_0 the chemical potential of the free electrons. We choose this form, rather than the Gaussian density of states of the hypercubic lattice, as it has a finite bandwidth.

Before considering in detail the methods of solving these equations, we look at the form of these equations in the low energy regime, where we can give them an interpretation in terms of renormalized quasiparticles. We assume that we can expand $\Sigma_\sigma(\omega)$ in powers of ω for small ω and retain terms to first order in ω only. Substituting this expansion into the equation for the local Green's function gives

$$G^{\mathrm{loc}}_\sigma(\omega) = z_\sigma \int d\varepsilon \frac{D(\varepsilon/z_\sigma)}{\omega + \tilde{\mu}_{0,\sigma} + \mathcal{O}(\omega^2) - \varepsilon}, \tag{9}$$

where

$$\tilde{\mu}_{0,\sigma} = z_\sigma[\mu_\sigma - \Sigma_\sigma(0)] \quad \text{and} \quad z_\sigma = 1/[1 - \Sigma'_\sigma(0)]. \tag{10}$$

We have assumed the Luttinger result that the imaginary part of the self-energy vanishes at $\omega = 0$. As the Green's function in Eq. (9) has the same form as in the noninteracting system, apart from the weight factor z_σ, we can use it to define a free quasiparticle propagator, $\tilde{G}^{\mathrm{loc}}_{0,\sigma}(\omega)$,

$$\tilde{G}^{\mathrm{loc}}_{0,\sigma}(\omega) = \int d\varepsilon \frac{D(\varepsilon/z_\sigma)}{\omega + \tilde{\mu}_{0,\sigma} - \varepsilon}. \tag{11}$$

We then interpret z_σ as the quasiparticle weight. We will refer to the density of states $\tilde{\rho}_{0,\sigma}(\omega)$ derived from this Green's function via $\tilde{\rho}_{0,\sigma}(\omega) = -\mathrm{Im}\,\tilde{G}_{0,\sigma}(\omega + i\delta)/\pi$ as the free quasiparticle density of states (DOS). For the Bethe lattice, the quasiparticle DOS takes the form of a band with renormalized parameters,

$$\tilde{\rho}_{0,\sigma}(\omega) = \frac{2}{\pi \tilde{D}^2_\sigma}\sqrt{\tilde{D}^2_\sigma - (\omega + \tilde{\mu}_{0,\sigma})^2}, \tag{12}$$

where $\tilde{D}_\sigma = z_\sigma D$. We can also define a quasiparticle occupation number $\tilde{n}^0_\sigma$ by integrating this density of states up to the Fermi level,

$$\tilde{n}^0_\sigma = \int_{-\infty}^{0} d\omega \tilde{\rho}_{0,\sigma}(\omega). \tag{13}$$

With a generalization of Luttinger's theorem[18] for each spin component, it is possible to relate this free quasiparticle occupation number $\tilde{n}^0_\sigma$ to the expectation value of the occupation number n_σ in the interacting system at $T=0$. Using the quasiparticle density of states in Eq. (12), we can rewrite Eq. (13) as

$$\tilde{n}^0_\sigma = \int_{-\infty}^{\infty} d\varepsilon D(\varepsilon)\theta[\mu_\sigma - \Sigma_\sigma(0) - \varepsilon], \tag{14}$$

where $\theta(\varepsilon)$ is the Heaviside step function and $D(\varepsilon)$ as given in Eq. (8). Assuming Luttinger's result for each spin compo-

nent, the right-hand side of Eq. (14) is equal to n_σ. We then have the result,

$$\tilde{n}^0_\sigma = n_\sigma, \tag{15}$$

that the occupation for electrons of spin σ is equal to the number of free quasiparticle of spin σ, as calculated from Eq. (13). It should be noted that there is no simple generalization of the $h=0$ result, $\mu-\mu_0=\Sigma(0)$, in the spin polarized case.

To solve the DMFT equations, we need an impurity solver, and the most commonly used are the quantum Monte Carlo, the exact diagonalization (ED) method, and the NRG, all of which have advantages and disadvantages. Here, we use the NRG approach as it is the most accurate method for calculations at $T=0$ and for the low energy excitations. There has been a DMFT study of the static properties of a half-filled Hubbard model in a magnetic field using the ED method by Laloux *et al.*[7] The focus of our paper here, however, is rather different so there is little overlap with this earlier work but, where there is, we make comment and compare with their results.

To evaluate the renormalized parameters, z_σ and $\mu_{0,\sigma}$, which specify the form of the quasiparticle DOS, we use two different methods based on the NRG approach. The first method is a direct one, where we use the NRG to determine the self-energy $\Sigma_\sigma(\omega)$ and the chemical potential μ_σ, and then substitute into Eq. (10) for z_σ and $\tilde{\mu}_{0,\sigma}$. The second method is indirect and makes no reference to the self-energy. It is based on the quasiparticle interpretation of the NRG low energy fixed point of the effective impurity. To explain this approach, we need to consider in a little detail how the NRG calculations are carried out.

In the NRG approach,[19] the conduction band is logarithmically discretized and the model then converted into the form of a one-dimensional tight-binding chain, coupled via an effective hybridization V_σ to the impurity at one end. In this representation, $K_\sigma(\omega)=|V_\sigma|^2 g_{0,\sigma}(\omega)$, where $g_{0,\sigma}(\omega)$ is the one-electron Green's function for the first site of the isolated conduction electron chain. As earlier, we expand the self-energy $\Sigma_\sigma(\omega)$ to first order in ω, and then substitute the result into Eq. (7). We then define a free quasiparticle propagator, $\tilde{G}_{0,\sigma}(\omega)$, for the impurity site as

$$\tilde{G}_{0,\sigma}(\omega) = \frac{1}{\omega - \tilde{\varepsilon}_{d\sigma} - |\tilde{V}_\sigma|^2 g_{0,\sigma}(\omega)}, \tag{16}$$

where

$$\tilde{\varepsilon}_{d\sigma} = z_\sigma[\varepsilon_{d\sigma} + \Sigma_\sigma(0)], \quad |\tilde{V}_\sigma|^2 = z_\sigma |V_\sigma|^2. \tag{17}$$

In the DMFT approach, we identify $\tilde{G}_{0,\sigma}(\omega)$ with the local quasiparticle Green's function for the lattice [Eq. (11)],

$$\tilde{G}^{\rm loc}_{0,\sigma}(\omega) = \tilde{G}_{0,\sigma}(\omega), \tag{18}$$

which specifies the form of $g_{0,\sigma}(\omega)$ in Eq. (16) and yields $\tilde{\mu}_{0,\sigma}=-\tilde{\varepsilon}_{d\sigma}$. By fitting the low energy single-particle excitations found in the NRG results to the poles of this Green's function, we can deduce the parameters $\tilde{\varepsilon}_{d\sigma}$ and $\tilde{V}_\sigma$, as has been explained in an earlier work.[20] The quasiparticle weight z_σ is then obtained from the relation $z_\sigma=|\tilde{V}_\sigma/V_\sigma|^2$ in Eq. (17), and $\tilde{\mu}_{0,\sigma}$ from $\tilde{\mu}_{0,\sigma}=-\tilde{\varepsilon}_{d\sigma}$.

Using the DMFT-NRG approach, we can calculate the spectral densities for the local two-particle response functions as well as single-particle ones. The main interest here will be in the local longitudinal and transverse dynamic spin susceptibilities, $\chi_l(\omega)$ and $\chi_t(\omega)$. Having calculated the renormalized parameters, which describe the free quasiparticles, we can compare the DMFT-NRG results for the dynamic susceptibilities with the corresponding quantities calculated via a renormalized RPA-like treatment that takes account of repeated quasiparticle-quasihole scattering. This approach has been described fully elsewhere for the Anderson impurity model.[11,14] The calculations here proceed along similar lines as for the effective impurity model. The equation for the transverse susceptibility is

$$\chi_t(\omega) = \frac{\tilde{\chi}_{\uparrow\downarrow}(\omega)}{1 - \tilde{U}_t(h)\tilde{\chi}_{\uparrow\downarrow}(\omega)}, \tag{19}$$

where $\tilde{\chi}_{\uparrow\downarrow}(\omega)$ is the transverse susceptibility calculated using the free quasiparticle density of states given in Eq. (12), and $\tilde{U}_t(h)$ is the irreducible quasiparticle interaction in this channel. For the Anderson model, it was possible to calculate $\tilde{U}_t(h)$ in terms of the renormalized on-site interaction $\tilde{U}$. Though it is possible in the lattice case to calculate $\tilde{U}$, we have no way of deducing $\tilde{U}_t(h)$ from it since unlike in the impurity case we do not have an exact expression for $\chi_t(0)$ in terms of $\tilde{U}$. We determine it to fit the DMFT-NRG result for Re $\chi_t(\omega)$ at the single point $\omega=0$. The corresponding result for the longitudinal susceptibility $\chi_l(\omega)$ is

$$\chi_l(\omega) = \frac{\tilde{\chi}_{\uparrow\uparrow}(\omega,h) + \tilde{\chi}_{\downarrow\downarrow}(\omega,h) + 4\tilde{U}_l(h)\tilde{\chi}_{\uparrow\uparrow}(\omega,h)\tilde{\chi}_{\downarrow\downarrow}(\omega,h)}{2[1 - 4\tilde{U}_l^2(h)\tilde{\chi}_{\uparrow\uparrow}(\omega,h)\tilde{\chi}_{\downarrow\downarrow}(\omega,h)]}, \tag{20}$$

where the susceptibilities $\tilde{\chi}_{\sigma\sigma}(\omega)$ are those for the free quasiparticles, and $\tilde{U}_l(h)$ is determined by fitting the DMFT-NRG result for Re $\chi_l(0)$.

Having covered the basic theory, we are now in a position to survey the results for the Hubbard model in different parameter regimes.

III. RESULTS AT HALF-FILLING

We present the results at half-filling for three main parameter regimes where we find qualitatively different behaviors. The results in all cases will be for a Bethe lattice with a bandwidth $W=2D=4$, setting $t=1$ as the energy scale. The local spectral densities are calculated from Eq. (3) using the NRG deduced self-energy.[21] In the evaluation of all NRG spectra, we use the improved method[22,23] based on the complete Anders-Schiller basis.[24] In concentrating on the field induced polarization, we do not include the possibility of antiferromagnetic ordering. The regimes are (a) a relatively weak coupling regime where U is smaller than the bandwidth, (b) an intermediate coupling regime with $W<U$

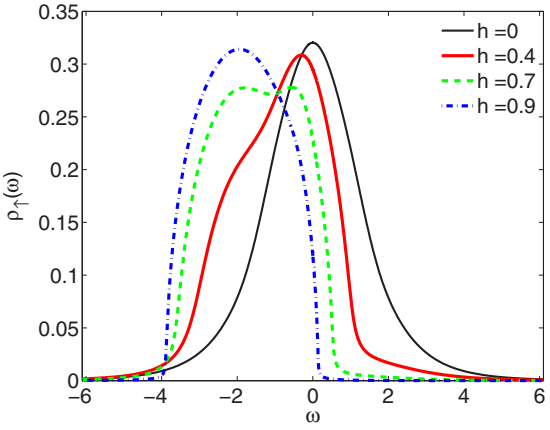

FIG. 1. (Color online) The local spectral density for the majority spin $\rho_\uparrow(\omega)$ for $U=2$ and various fields h.

$<U_c$, where U_c is the value at which a Mott-Hubbard gap develops in the absence of a magnetic field ($U_c \approx 5.88$),[25] and (c) a strong coupling regime with $U>U_c$.

A. Weakly correlated regime

The first plot in Fig. 1 gives the spectral densities for the majority spin electrons $\rho_\uparrow(\omega)$ for various magnetic field values in the weakly correlated regime, $U=2$. We can clearly see that, for increasing magnetic field, more and more spectral weight is shifted to lower energies (the opposite happens for the other spin component, which is not displayed here). Above $h \simeq 1.0$, the system is completely polarized, $2m=1$. This extreme high field limit corresponds to a band insulator. There is a gap of the magnitude $\Delta_g(h)=2h+U-W$ between the upper (minority) and lower (majority) bands, which both have the semielliptical form as for the noninteracting system with $W=4$. At this point, dynamic renormalization effects have vanished. The inverse of the quasiparticle weight $z_\sigma(h)$, which corresponds to the enhancement of the effective mass $m^*_\sigma(h)=m/z_\sigma(h)$, is shown as a function of h in Fig. 2. We

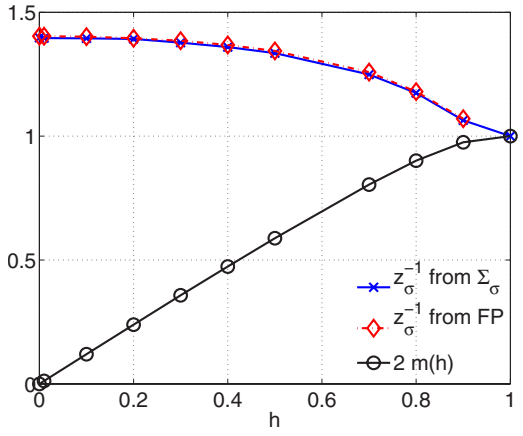

FIG. 2. (Color online) The inverse of the quasiparticle weight $z_\sigma(h)$ calculated from the impurity fixed point (FP) and directly from the self-energy and the magnetization $m(h)$ for $U=2$ and various fields h.

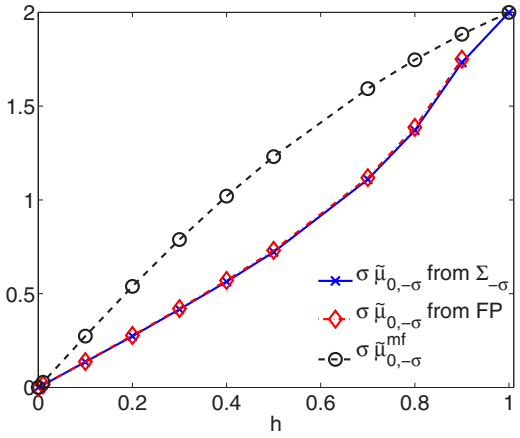

FIG. 3. (Color online) The renormalized chemical potential $\tilde{\mu}_{0,\sigma}(h)$ calculated from the impurity fixed point (FP) and directly from the self-energy for $U=2$ and various fields h.

calculated the values of $z_\sigma(h)$ using the two methods described earlier. At half-filling, we have $z_\uparrow(h)=z_\downarrow(h)$ and we have plotted the average of the values for $\sigma=\uparrow$ and $\sigma=\downarrow$, which is compared for the two methods. The deviation for the values for the different spins is only due to small numerical inaccuracies and is less than 2%. The method based on analyzing the excitations of the impurity fixed point (FP) is only applicable in the metallic regime and when the system is not completely polarized. From these results shown in Fig. 2, it can be seen that the two sets of values are in good agreement. The values of $z_\sigma(h)$ increase from about 0.75 to 1, which corresponds to a progressive "derenormalization" of the quasiparticles with increasing field, as observed earlier for the impurity model.[10] Since the interaction term in the Hubbard model acts only for opposite spins, it is clear that there is no renormalization when the system is completely polarized with one band fully occupied and the other empty. The expectation value of the double occupancy $\langle n_\uparrow n_\downarrow \rangle$ decreases with increasing field, which further illustrates why the interaction term becomes less important for larger fields.

We can also follow the field dependence of the renormalized chemical potential $\tilde{\mu}_{0,\sigma}(h)$, as plotted in Fig. 3. In the case of particle-hole symmetry, we have $\tilde{\mu}_{0,\uparrow}(h)=-\tilde{\mu}_{0,\downarrow}(h)$, and similar to the case for the quasiparticle weight we have displayed the average of the up and down spin values for each method. Also, here the deviation within one method is only due to small numerical inaccuracies and less than 2%.

Again, the agreement between the two methods of calculation is very good over the full range of magnetic fields. Mean-field theory is valid for very weak interactions, so we compare our results for $\tilde{\mu}_{0,\sigma}(h)$ for $U=2$ with the mean-field value $\tilde{\mu}^{\mathrm{MF}}_{0,\sigma}=\mu+\sigma h-Un^{\mathrm{MF}}_{-\sigma}$ in Fig. 3. The results coincide for $h=0$, when $\tilde{\mu}^{\mathrm{MF}}_{0,\sigma}=0$ and when the system becomes fully polarized at large field values, $\tilde{\mu}^{\mathrm{MF}}_{0,\sigma}=-\sigma(U+h)$, but in general $\tilde{\mu}^{\mathrm{MF}}_{0,\sigma}>\tilde{\mu}_{0,\sigma}(h)$. We also compare the mean-field (MF) result for the field dependence of the magnetization $m(h)$ with the one obtained in the DMFT calculation in Fig. 4. The general behavior is similar, but the mean-field theory without quantum fluctuations overestimates the magnetization, as one would expect.

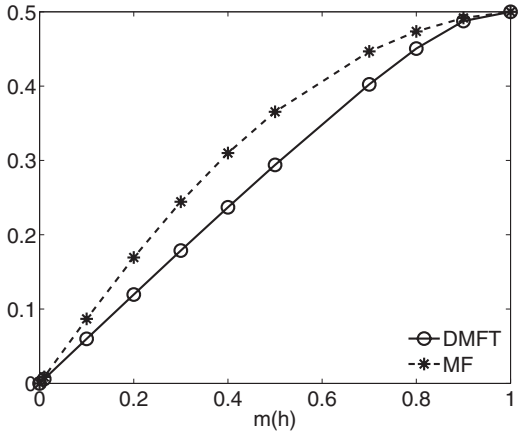

FIG. 4. The magnetization in the mean-field approximation compared with the DMFT result for $U=2$ and for the full range of magnetic fields h.

B. Intermediate coupling regime

In the next plot in Fig. 5, where $U=5$, we show typical behavior of the local spectral density in the intermediate coupling regime.

Similar to the weak coupling regime, we find a shift of spectral weight towards lower energy for the majority spin. There is, however, a difference in the way this happens due to the initial three peak structure, namely, the quasiparticle peak in the middle gets narrower for increasing field and finally vanishes in the polarized phase. The quasiparticle weight, which is shown in Fig. 6, reflects this behavior by decreasing to zero with increasing field signaling heavy quasiparticles. Here, as in the weak coupling case, we plot the average of the spin up and down results for each method. The deviations can be larger here, especially close to the metamagnetic transition.

When the material is polarized, $z_\sigma(h)$ reverts to 1, which corresponds to the band insulator as before. This approach to the fully polarized localized state in high fields contrasts with that found in the weak coupling regime. It gives rise to the metamagnetic behavior in this parameter regime. To illustrate further the different response to a magnetic field, the real part of the local longitudinal dynamic spin susceptibility

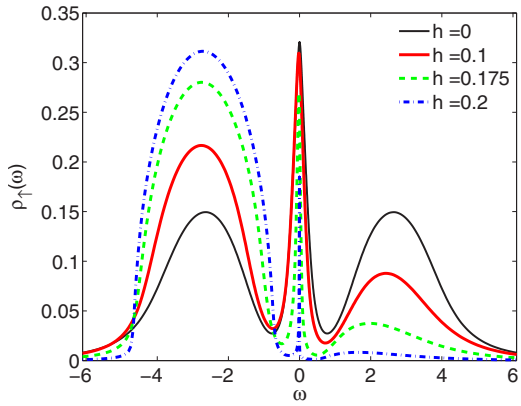

FIG. 5. (Color online) The local spectral density for the majority spin $\rho_\uparrow(\omega)$ for $U=5$ and various fields h.

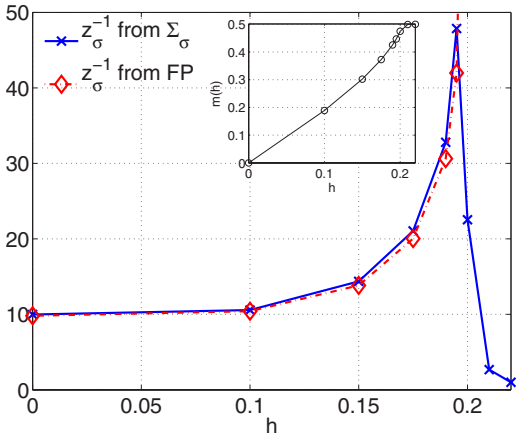

FIG. 6. (Color online) The inverse of the quasiparticle weight $z_\sigma(h)$ calculated from the impurity fixed point (FP) and directly from the self-energy for $U=5$ and various fields h. The inset shows the magnetization $m(h)$.

$\chi_l(\omega,h)$ as a function of ω is shown for various values of h in Fig. 7. It can be seen that the local susceptibility $\chi^{\mathrm{loc}}(h)=\mathrm{Re}\,\chi_l(0,h)$ in this regime increases with h so that $\partial\chi^{\mathrm{loc}}(h)/\partial h>0$. This can also be seen in the curvature of the magnetization shown in the inset of Fig. 6. This behavior is characteristic of a metamagnetic transition and related to the magnetic field induced metal-insulator transition. Laloux *et al.*[7] find the metamagnetic behavior in a similar parameter regime. There, a comparison is made with results from the Gutzwiller approximation, which gives such a behavior already for smaller values of the interaction, and we refer to their paper for details.

We can also check the Luttinger theorem in a magnetic field [Eq. (15)] by comparing the values of $\tilde{n}_\sigma^0$, deduced from integrating the quasiparticle density of states, with the value of n_σ calculated from the direct NRG evaluation in the ground state. The results are shown in Fig. 8. It can be seen that there is excellent agreement between the results of these two different calculations, $\tilde{n}_\sigma^0=n_\sigma$, so that Luttinger's theorem is satisfied for all values of the magnetic field in this intermediate coupling regime.

Having deduced the renormalized parameters of the quasiparticles from the NRG results, we are now in a position to

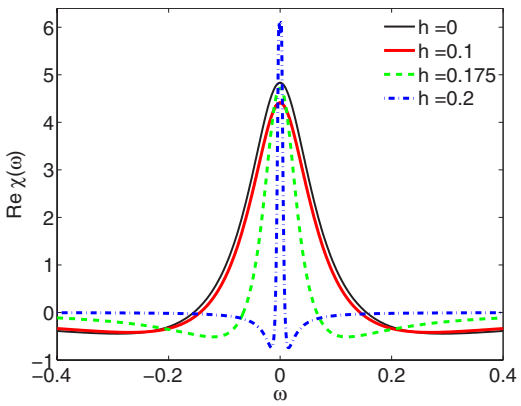

FIG. 7. (Color online) The real part of the local longitudinal dynamic spin susceptibility for $U=5$ and various fields h.

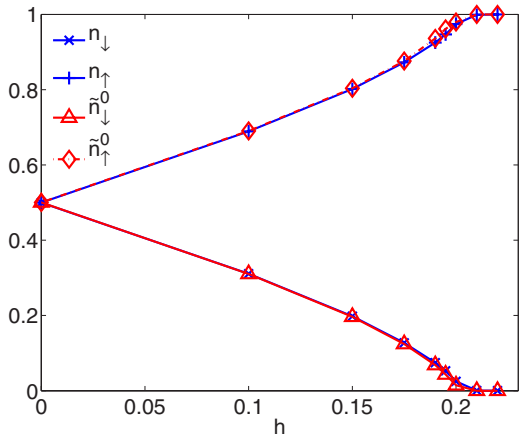

FIG. 8. (Color online) The comparison of the spin dependent occupation numbers $\tilde{n}_\sigma^0$ and n_σ corresponding to Luttinger's theorem in a magnetic field for $U=5$ and the range of fields h.

test how well we can describe the low energy dynamics of this model in a magnetic field in terms of a renormalized perturbation theory. It is of interest first of all to see how the free quasiparticle density of states $\tilde{\rho}_{0,\sigma}(\omega)$ multiplied by $z_\sigma(h)$ compares with the full spectral density $\rho_\sigma(\omega)$. In Fig. 9 (upper panel), we make a comparison in the zero magnetic field case.

We see that the quasiparticle band gives a good representation of the low energy peak in $\rho_\sigma(\omega)$ and, as expected, does not reproduce the high energy features. These, however, to a fair approximation can be described by the mean-field solution $\rho_{\mathrm{MF}}(\omega)$ weighted with a factor $1-z_\sigma$, as can be seen in Fig. 9 (upper panel). A case with a finite magnetic field $h=0.15$, where the peaks in the density of states of the two spin species are shifted due to the induced polarization relative to the Fermi level, is shown in Fig. 9 (lower panel). The figure focuses on the region at the Fermi level and one can see that the free quasiparticle density of states describes well the form of $\rho_\sigma(\omega)$ in the immediate vicinity of the Fermi level. It is to be expected that the frequency range for this agreement can be extended if self-energy corrections are included in the quasiparticle density of states using the renormalized perturbation theory as shown in the impurity case.[26]

We now compare the NRG results for the longitudinal and transverse local dynamic spin susceptibilities for the same value $U=5$ and a similar range of magnetic field values with those based on RPT formulas (20) and (19). In Fig. 10 (upper panel), we show the imaginary part of the transverse spin susceptibility calculated with the two different methods.

It can be seen that the RPT formula gives the overall form of the NRG results and precisely fits the gradient of the NRG curve at $\omega=0$. Some of the relatively small differences between the results might be attributed to the broadening factor used in the NRG results which gives a slower falloff with ω in the higher frequency range and a slightly reduced peak. We get similar good agreement between the two sets of results for the same quantity for the case with a magnetic field $h=0.15$, shown in Fig. 10 (lower panel).

In Fig. 11, where we give both the real and imaginary parts of the transverse susceptibility for $h=0.19$, we see that

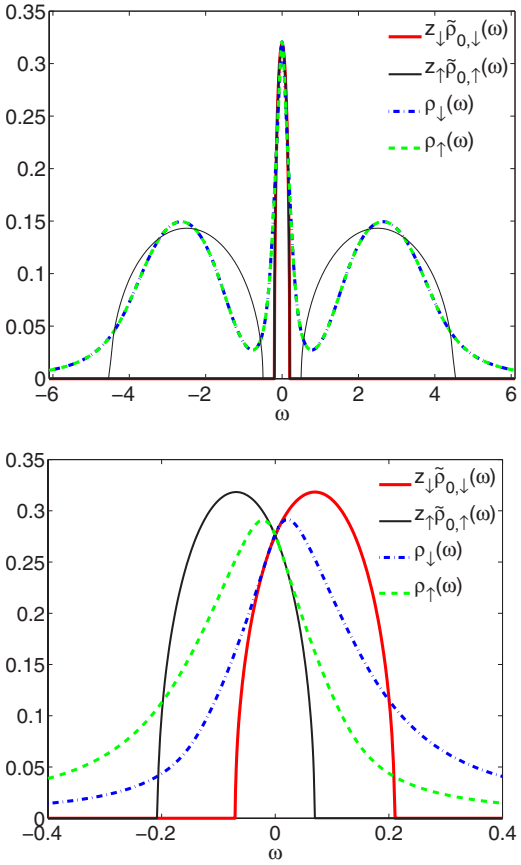

FIG. 9. (Color online) The free quasiparticle density of states in comparison with interacting local spectral density for $U=5$ and $h=0$ (upper panel). We have also plotted a thin black line for $\rho_{\mathrm{MF}}(\omega)=[D(\omega+U/2)+D(\omega-U/2)]/2$ which describes the nonmagnetic mean-field solution and weighted with $1-z_\sigma$. In the lower panel, we have a similar comparison for $U=5$ and $h=0.15$ concentrating on low energies.

this overall agreement is maintained in the large field regime where we get the metamagnetic behavior. The shapes of the low energy peaks for both quantities are well reproduced by the RPT formulas. Note that the peak in the real part is not at $\omega=0$, so it is not fixed by the condition that determines $\tilde{U}_t$, but nevertheless is in good agreement with the NRG results. Due to their very small values, it becomes difficult to calculate $z_\sigma(h)$ as the system approaches localization for larger fields. In this regime, as $z_\sigma(h)\to 0$ the free quasiparticle density of states will converge to a delta function. Self-energy corrections to the free quasiparticle propagators, which were used in the calculation of $\tilde{\chi}_{\sigma,\sigma'}(\omega)$, will become increasingly important as this limit is approached. Once the system has undergone the localization transition and is completely polarized, however, we find that the values $\tilde{\mu}_\sigma$ $[z_\sigma(h)=1]$ deduced from the self-energy give a quasiparticle density of states coinciding with the DMFT-NRG result of an upper and lower semicircular bands.

Results for the longitudinal susceptibility are shown in Figs. 12 and 13. In Fig. 12, we give the values for the real part as a function of ω for $h=0$ and $h=0.15$. Here the peak height, which is at $\omega=0$, is fixed by the condition which

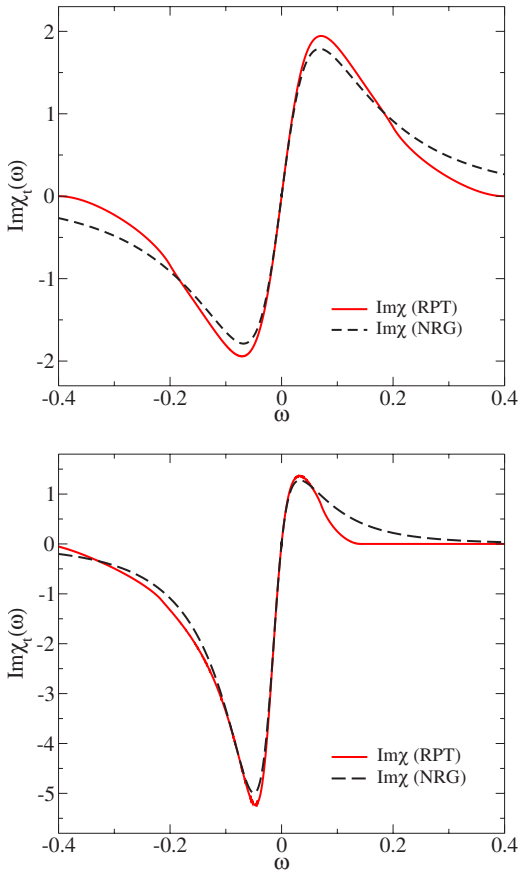

FIG. 10. (Color online) A comparison of the imaginary parts of the transverse dynamic spin susceptibility for $U=5$ and $h=0.0$ (upper panel) and $h=0.15$ (lower panel) calculated using renormalized perturbation theory (RPT) (full line) and from a direct NRG calculation (dashed line).

determines $\tilde{U}_l$. The widths of the peaks in the two sets of NRG results, however, are given reasonably well by the RPT equations. The imaginary part of the longitudinal susceptibility obtained by the two methods is given in Fig. 13 for $h=0.15$. Again, there is overall agreement between the two sets of results. The slight undulations seen in the RPT results

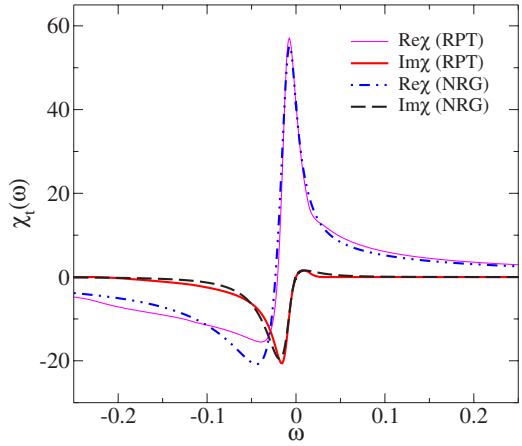

FIG. 11. (Color online) The real and imaginary parts of the transverse dynamic spin susceptibility for $U=5$ and $h=0.19$.

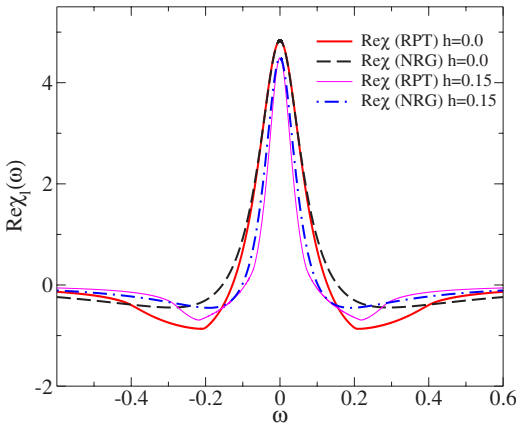

FIG. 12. (Color online) The real part of the longitudinal dynamic spin susceptibility for $U=5$ and $h=0$ and $h=0.15$.

are due to the sharp cutoff in the band edges in the free quasiparticle density of states. For larger values of h, the agreement with the NRG results is not as good as that as for the transverse susceptibility, and the central peak in the real part of the RPT results narrows more rapidly with h than in those obtained from the direct NRG calculation.

C. Strong coupling regime

Finally, we consider the strong coupling regime with $U > U_c$, where for $h=0$ the spectral density has a Mott-Hubbard gap so that for half-filling the system is an insulator. The electrons will be localized with free magnetic moments coupled by an effective antiferromagnetic exchange $J \sim t^2/U$. In fields such that $h > J$, the system polarizes completely, as can be seen in Fig. 14, where we show the total density of states $\rho(\omega)=\rho_\uparrow(\omega)+\rho_\downarrow(\omega)$ for $h=0$ and $h=0.2$.

For smaller fields, such that $h < J$, we do not find a convergent solution to the DMFT equations, and the iterations oscillate between local states which are either completely full or empty. We interpret this as due to the tendency to antiferromagnetic order which in a weak field, due to the absence of anisotropy, will be almost perpendicular to the applied field in the x-y plane with a slight canting of the spins in the z

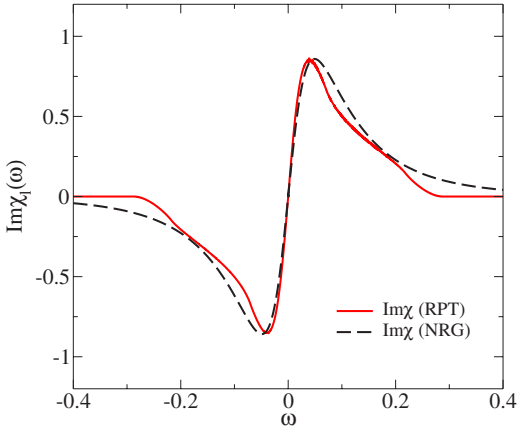

FIG. 13. (Color online) The imaginary part of the longitudinal dynamic spin susceptibility for $U=5$ and $h=0.15$.

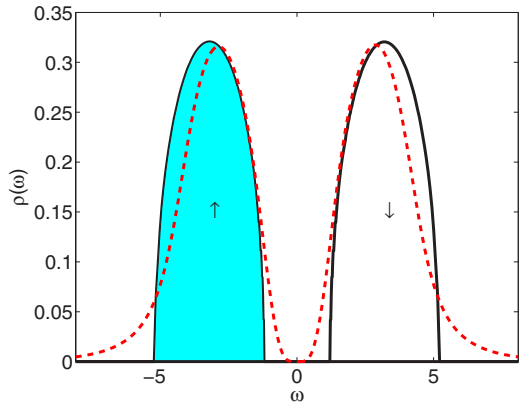

FIG. 14. (Color online) The total local spectral density $\rho(\omega)$ for $U=6$ for $h=0$ (dashed line), Mott insulator, and $h=0.2$ (full line), fully polarized band insulator.

direction (spin flopped phase). In this calculation, no allowance has been made for this type of ordering, but this state can be well described using an effective Heisenberg model for the localized moments.

IV. RESULTS AWAY FROM HALF-FILLING

After the extensive discussion of the behavior of the Hubbard model in a magnetic field at half-filling, we want to compare these results with the situation where the system is doped with holes. As is well known, doping retains the metallic character of the system and one does not find a paramagnetic metal-insulator transition anymore. Thus, we do not find distinct regimes (a)–(c) any longer. To illustrate the characteristics of the magnetic response for the doped system, we focus on two cases, one at quarter filling and one very close to half-filling.

A. Quarter filled case

First, we compare the results in the intermediate coupling regime with $U=5$ at half-filling with those at quarter filling, $x=0.5$. In the latter case, the Fermi level falls in the lower Hubbard peak in the spectral density. To see how the band changes with increasing magnetic field, we plot the density of states for both spin types, for the majority spin electrons (Fig. 15, upper panel) and for the minority spin electrons (Fig. 15, lower panel), for various values of the magnetic field.

In the majority spin case, the lower peak gains spectral weight on the low energy side and the weight in the upper peaks decreases with the increase of the field. For the fully polarized case ($h>0.4$), the Fermi level, which is indicated by a dotted line, lies in the middle of the lower band, which has the noninteracting semicircular shape. The opposite features can be seen in the minority spin case, with the spectral weight in the lower peak below the Fermi level decreasing and the weight in the upper peak increasing. Thus, the increase of spectral weight below the Fermi level for the majority spin electrons, and the decrease for the minority spin electrons, can be seen to be due to a change of band shape

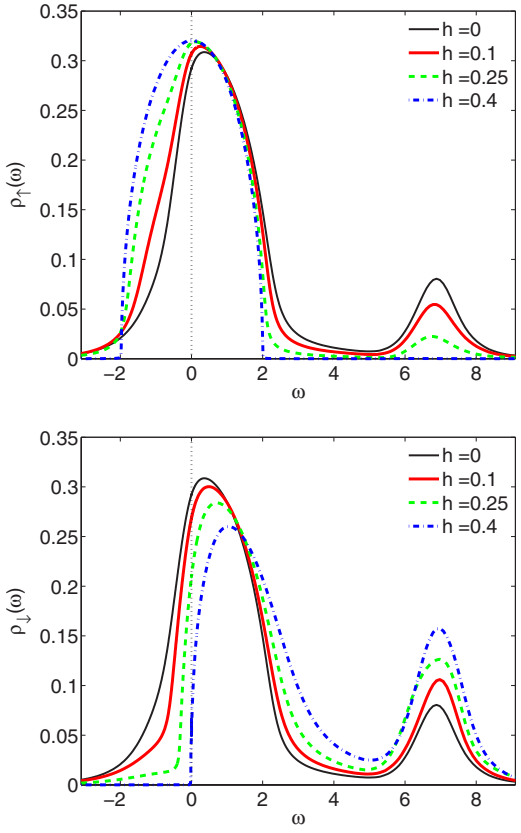

FIG. 15. (Color online) The local spectral density for the majority spin $\rho_\uparrow(\omega)$ (upper panel) and for the minority spin $\rho_\downarrow(\omega)$ (lower panel) for $U=5$, $x=0.5$, and various fields h.

rather than a simple relative shift of the two bands, which would be the case in mean-field theory. In the fully polarized state, there are no minority states below the Fermi level and the upper peak in the majority state density of states has disappeared.

The corresponding values for the inverse of the quasiparticle weight $1/z_\sigma(h)$ are shown in Fig. 16 for a range of fields. As noted in the impurity case,[11] the quasiparticle

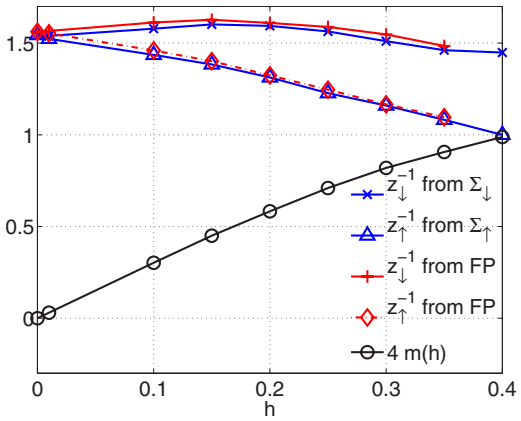

FIG. 16. (Color online) The inverse of the quasiparticle weight $z_\sigma(h)$ calculated from the impurity fixed point (FP) and directly from the self-energy for $U=5$, $x=0.5$, and various fields h. The magnetization $m(h)$ is also displayed.

weights differ for the two spin types with $z_\uparrow(h) > z_\downarrow(h)$. The values of $z_\sigma(h)$ have been calculated, as described earlier, both from the energy levels (FP) and from a numerical derivative NRG derived self-energy. There is reasonable agreement between the two sets of results, and the small differences can be attributed to the uncertainty in the numerical derivative of the NRG self-energy. As observed in the case for the nonsymmetric Anderson model,[11] there is an initial decrease of $z_\downarrow(h)$ with an increase of h, whereas $z_\uparrow(h)$ increases monotonically. This implies that the effective mass of the majority spin electrons decreases to its bare value, while the effective mass of the minority spin electrons does not decrease much. The reason for that is that in the polarized system, the up electrons cannot interact through the Hubbard interaction term, whereas a down spin electron can interact with all the up spin electrons leading to an enhanced mass. The field dependence of the magnetization is also shown in Fig. 16 and is similar to the half-filled case with a weak interaction ($U=2$). We have calculated, but do not show, the corresponding occupation values for $\tilde{n}_\sigma^0$ which again agree well with the values of $\tilde{n}_\sigma$, confirming Luttinger's theorem in a magnetic field.

We give two examples of results for the susceptibilities for this case. In Fig. 17 (upper panel), we plot the real and imaginary parts of the transverse susceptibility. Despite the large value of U, we can see that the peak heights are very much reduced compared with those seen in the half-filled case for $U=5$. The peak widths are also an order of magnitude larger as can be seen from the ω scale. The RPT results reproduce well the overall features to be seen in the NRG results, but we note some discrepancies in the shape of the curve at larger frequencies, where the RPT shows more pronounced features. The real and imaginary parts for the longitudinal susceptibility are shown in Fig. 17 (lower panel). Again all the low energy features are reproduced in the RPT results and differences are mainly seen for tails at larger energies. In this regime, apart from the overall factor of 2, there is less difference between the transverse and longitudinal susceptibilities than at half-filling.

Our conclusion from these results, and from calculations with other values of U at quarter filling, is that when there is significant doping, the behavior in the field corresponds to a weakly correlated Fermi liquid, very similar to that at half-filling in the weak interaction regime. The only remarkable difference in the presence of a magnetic field is the spin dependence of the effective masses, as shown in Fig. 16.

B. Near half-filling

Very close to half-filling and for large values of U, we have a qualitatively different parameter regime. Here, the system is metallic but we can expect strong correlation effects when U is of the order or greater than U_c due to the much reduced phase space for quasiparticle scattering. We look at the case with 5% hole doping from half-filling and a value $U=6$, which is just greater than the critical value for the metal-insulator transition. We show the spectral density of states for the majority spin state (Fig. 18, upper panel) and for the minority spin state (Fig. 18, lower panel) for various values of the magnetic field.

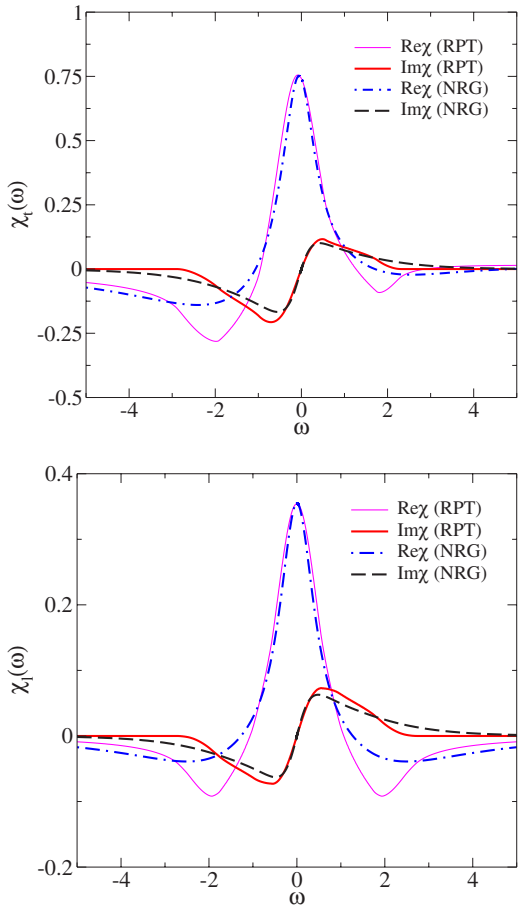

FIG. 17. (Color online) The real and imaginary parts of the transverse dynamic spin susceptibility (upper panel) and of the longitudinal dynamic spin susceptibility (lower panel) for $U=5$, $x=0.5$, and $h=0.1$.

There is a clear sharp quasiparticle peak for $h=0$ at the Fermi level (marked by a dotted line) at the top of the lower Hubbard band. As in the quarter filling case with $U=5$, we see a similar transfer of spectral weight with increasing field to below the Fermi level for the majority spin case and above the Fermi level for the minority spins. For large fields, when the system is completely polarized the Fermi level lies close to the top of the lower band in the majority spin spectrum. One can see in the lower panel that there is still a sharp narrow peak in the spectral density of the minority spin states above the Fermi level, though the spectrum for the majority states below the Fermi level is that of the noninteracting system. A spin up electron added above the Fermi level feels no interaction as the system is completely spin up polarized so these electrons see the noninteracting density of states. On the other hand, a spin down electron above the Fermi level interacts strongly with the sea of up spin electrons. The self-energy due to scattering with particle-hole pairs in the sea creates a distinct resonance in the down spin density of states just above the Fermi level. Just such a resonance was predicted by Hertz and Edwards[27] for a Hubbard model in a strong ferromagnetic (fully polarized) state.

The field dependence of the inverse of the quasiparticle weight is presented in Fig. 19. Again, we find reasonable

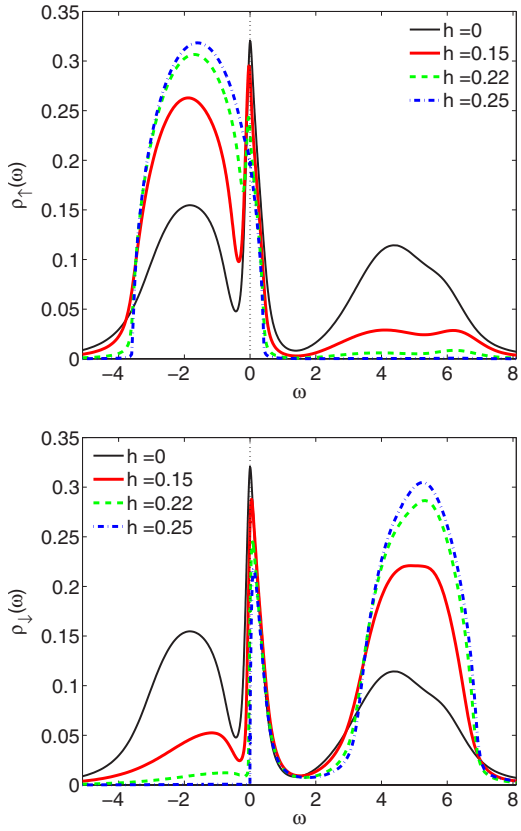

FIG. 18. (Color online) The local spectral density for the majority spin $\rho_{\uparrow}(\omega)$ (upper panel) and for the minority spin $\rho_{\downarrow}(\omega)$ (lower panel) for $U=6$, $x=0.95$, and various fields h.

agreement between the two methods of calculation for these quantities. The magnetization as a function of h is shown as an inset in the same figure. The behavior of $z_{\uparrow}(h)$ and $z_{\downarrow}(h)$ as a function of h contrasts sharply with the behavior found for the metallic state at half-filling with $U=5$ shown in Fig. 6. For zero field, the quasiparticle weight has a very similar value in both cases. At half-filling, the tendency of the magnetic field to induce localization resulted in values of $z_{\uparrow}(h)$

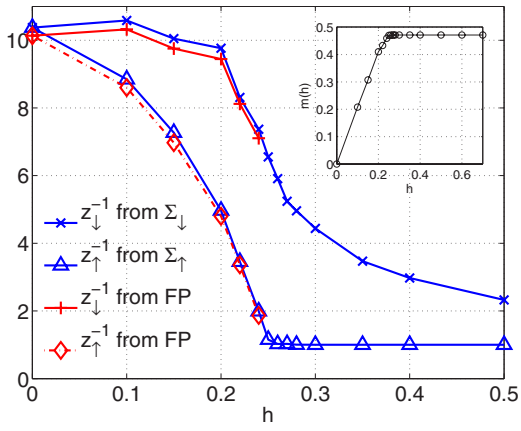

FIG. 19. (Color online) The inverse of the quasiparticle weight $z_{\sigma}(h)$ calculated from the impurity fixed point (FP) and directly from the self-energy for $U=6$, $x=0.95$, and various fields h. The inset shows the magnetization $m(h)$.

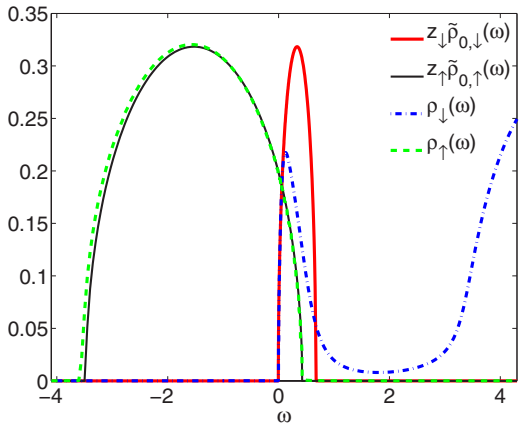

FIG. 20. (Color online) The free quasiparticle density of states in comparison with interacting local spectral density for $U=6$, $x=0.95$, and $h=0.26$.

and $z_{\downarrow}(h)$ $[z_{\uparrow}(h)=z_{\downarrow}(h)]$ which decrease sharply as a function of h. In the 5% doped case with $U=6$, the system must remain metallic and the quasiparticle weights, $z_{\uparrow}(h)$ and $z_{\downarrow}(h)$, both increase in large fields though their values differ significantly. The quasiparticle weight for the minority spin electrons decreases initially with the increase of h, whereas that for the majority spins $z_{\uparrow}(h)$ increases monotonically and quite dramatically with h. When the system becomes fully polarized ($h \simeq 0.26$), the up spin electrons become essentially noninteracting, $z_{\uparrow}(h)=1$, whereas there is a strong interaction for a down spin electron and we find in this case $z_{\downarrow}(h) \simeq 0.15$. The interpretation for this is as given in the previous paragraph for the spectral densities. On further increasing the magnetic field, $z_{\downarrow}(h)$ also tends to 1, but relatively slowly, as can be seen in Fig. 19. Note that the results in this regime are based on the calculation from the self-energy, as the method based on the fixed point analysis becomes difficult to apply in this regime.

Laloux *et al.*[7] compared the quasiparticle weight at half-filling for the infinite-dimensional model with results from the Gutzwiller approximation. The values for the infinite-dimensional model were found to be significantly smaller than the Gutzwiller predictions; the ratio is more than a factor of 2 for $U>4$ and zero field. Spałek and co-workers[4,28] have made predictions based on the Gutzwiller approach for situations away from half-filling in finite field, $z_{\uparrow} \neq z_{\downarrow}$. As in the study of Laloux *et al.*,[7] our results for $z_{\uparrow}$ and $z_{\downarrow}$ are significantly smaller than the Gutzwiller predictions.

For the fully polarized case ($h=0.26$), we show the comparison of the weighted free quasiparticle density of states $z_{\sigma}\tilde{\rho}_{0,\sigma}(\omega)$ with the full spectrum $\rho_{\sigma}(\omega)$ in Fig. 20. Note that the parameters $\tilde{\mu}_{0,\sigma}$ and z_{σ} in $\tilde{\rho}_{0,\sigma}(\omega)$ are purely derived from the NRG self-energy in this case. We can see that the different values for the field-dependent quasiparticle weight $z_{\sigma}(h)$ for up and down spins lead to remarkably different quasiparticle band shapes. With $z_{\uparrow} \simeq 1$, the majority spin quasiparticle band is essentially that of the noninteracting density of states. The very much smaller value $z_{\downarrow}$ leads to a narrow quasiparticle band above the Fermi level. The low energy flank of this quasiparticle band describes well the narrow

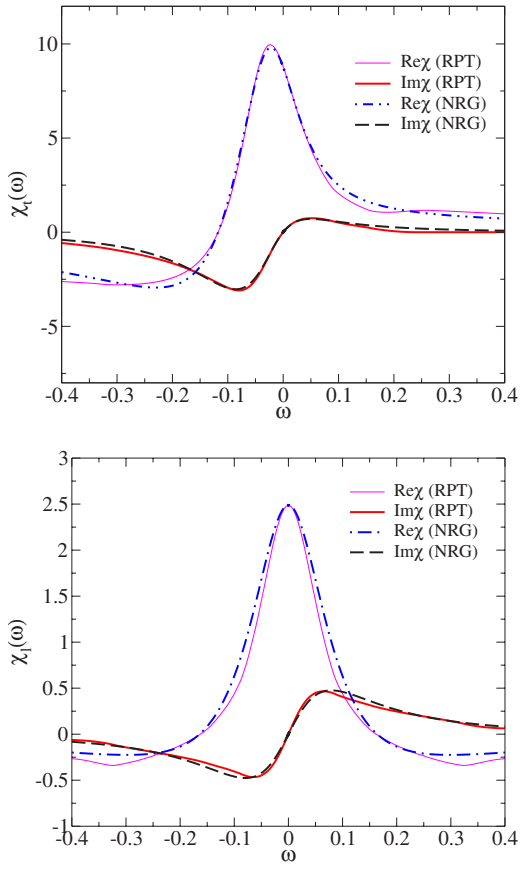

FIG. 21. (Color online) The real and imaginary parts of the transverse dynamic spin susceptibility (upper panel) and of the longitudinal dynamic spin susceptibility (lower panel) for $U=6$, $x=0.95$, and $h=0.15$.

peak seen in the spectral density just above the Fermi level. To describe these strong asymmetries in the spectral densities near half-filling, we need $z_\uparrow \gg z_\downarrow$, which contrasts with the cases at half-filling such as in Fig. 9 where always $z_\uparrow = z_\downarrow$. This suggests a discontinuous behavior of the renormalization factors z_σ on the approach to half-filling.

Also for this case, we show plots for the two susceptibilities for a field of $h=0.15$. In Fig. 21 (upper panel), we give the real and imaginary parts of the transverse susceptibility. The low energy features are seen on an ω scale an order of magnitude smaller than that for quarter filling due to the much stronger renormalization effects in this regime. There is excellent agreement both with the peak positions and shapes between the NRG and RPT results for both quantities. This is also seen to be the case for the real and imaginary parts of the longitudinal susceptibility shown in Fig. 21 (lower panel), though the peak in the real part can be seen to be marginally narrower in the RPT results.

At the end of this section, we conclude that already a small doping of the system is enough to maintain a metallic character even for very strong interaction. Although the zero field spectra of the half-filled case for $U=5$ and the small doping case with $U=6$ display very similar zero field behavior, i.e., a strongly renormalized quasiparticle band with similar z_σ, no field induced localization transition occurs for finite doping and no metamagnetic behavior is observed in the latter case.

V. SUMMARY

In this paper, we have used the DMFT-NRG method to calculate the spectral densities for one-particle and two-particle response functions for the infinite-dimensional Hubbard model in a magnetic field, for the qualitatively different filling regimes and interaction strengths. The results extend earlier calculations of Laloux *et al.*[7] using the ED method, which were restricted to the case of half-filling. Our results there are on the whole consistent with this earlier work, except in the insulating regime for weak fields, where we could not find a convergent solution of the DMFT equations. We attributed this to the fact that in this regime, the magnetic field is smaller than the exchange coupling between the localized spins so that the ground state would be one in which the spins would have a canted antiferromagnetic ordering in the plane perpendicular to the field.

Well away from half-filling, we find a magnetic response similar to the weakly correlated case even for large values of U. The large phase space for quasiparticle scattering in this regime leads to modest renormalization effects. Here, we find spin dependent quasiparticle weights, $z_\uparrow(h) \neq z_\downarrow(h)$. This implies spin dependent as well as field-dependent effective masses, which have been discussed earlier in the works of Spałek and co-workers[4,28] and Riseborough.[29] The calculations by Spałek and co-workers were based on a Gutzwiller[28] and a mean-field slave boson approach.[4] We can make a comparison of our results (Sec. VI B) near half-filling, $x=0.95$, with theirs in the later work.[4] We find a qualitatively similar behavior with the majority spin effective mass decreasing with h, but quantitatively there are differences. The field dependence of the minority spin effective mass $1/z_\downarrow(h)$ shows a very slow increase initially in both sets of results, but the large field behavior is quite different. As seen in Fig. 19, we find a significant decrease in $1/z_\downarrow(h)$ for large fields, whereas the corresponding quantity in Fig. 3 in Ref. 4 increases.

The strong magnetic field dependence of the effective masses found in the calculations by Riseborough is based on the assumption that the system is close to a ferromagnetic transition (paramagnon theory). However, DMFT calculations for the Hubbard model find that any ferromagnetism in the Hubbard model only occurs in a very small region of the parameter space near half-filling and for very large values of U.[30] Our results are well away from this regime and the large effective masses obtained here can be attributed to the tendency to localization rather than the tendency to ferromagnetism.

Using the field-dependent renormalized parameters $z_\sigma(h)$ and $\tilde{\mu}_{0,\sigma}(h)$ in the RPT formulas for the dynamic local longitudinal and transverse spin susceptibilities, we found agreement with the overall features to be seen in the DMFT-NRG results for these quantities. In the case of the transverse spin susceptibility, excellent agreement was found in all the metallic regimes and for all values of the magnetic field considered, except in the high field regime at half-filling as the localization point is approached, where consistent values of the renormalized parameters are difficult to calculate. The comparison of the RPT results with those from NRG was

also excellent for the longitudinal dynamic susceptibility in the weaker field regime $h \leqslant 0.15$ but less good for higher fields, $h > 0.15$.

In all metallic parameter regimes, a spin dependent Luttinger theorem in the form $n_\sigma = \tilde{n}^0_\sigma$, the number of particles equals the number of quasiparticles, was found to be satisfied for all strengths of the magnetic field. In this form, it even holds in the fully polarized insulating state.

Phenomena such as field-dependent and spin dependent effective masses and metamagnetic behavior have been observed experimentally in several heavy fermion compounds.[2,3,5,31] The Hubbard model, however, being a one band model is not an appropriate starting point to make a quantitative comparison with the heavy fermion class of materials. A periodic Anderson model with a two band structure and including the degeneracy of the f electrons would be a better model to describe these materials. Field-dependent effects in this model have been studied by several techniques, modified perturbation theory,[32] exact diagonalization,[33] $1/N$ expansion,[34] and variational approach.[35] The approach used here could be generalized to the periodic Anderson model but restricted to the nondegenerate case and $N=2$ as it is computationally too demanding in the NRG to deal with higher degeneracy. The Hubbard model at half-filling has been used as a lattice model to describe the strongly renormalized Fermi liquid ^{3}He.[6,7] However, the metamagnetic behavior predicted for relevant parameter regime is not seen experimentally.[36] In Sec. VI B, we found for small doping large effective masses but no metamagnetic behavior. This raises the possibility that the weakly doped Hubbard model could serve as a basis for interpreting the experimental results for liquid ^{3}He.

ACKNOWLEDGMENTS

We wish to thank N. Dupuis, D. M. Edwards, W. Koller, D. Meyer, and A. Oguri for helpful discussions and W. Koller and D. Meyer for their contributions to the development of the NRG programs. One of us (J.B.) thanks the Gottlieb Daimler and Karl Benz Foundation, the German Academic Exchange Service (DAAD), and the EPSRC for financial support.

[1] W. Joss, J. M. van Ruitenbeek, G. W. Crabtree, J. L. Tholence, A. P. J. van Deursen, and Z. Fisk, Phys. Rev. Lett. **59**, 1609 (1987).
[2] R. G. Goodrich, N. Harrison, A. Teklu, D. Young, and Z. Fisk, Phys. Rev. Lett. **82**, 3669 (1999).
[3] H. Aoki, S. Uji, A. K. Albessard, and Y. Onuki, Phys. Rev. Lett. **71**, 2110 (1993).
[4] P. Korbel, J. Spałek, W. Wójcik, and M. Acquarone, Phys. Rev. B **52**, R2213 (1995).
[5] M. Manekar, S. Chaudhary, M. K. Chattopadhyay, K. J. Singh, S. B. Roy, and P. Chaddah, J. Phys.: Condens. Matter **12**, 9645 (2000).
[6] D. Vollhardt, Rev. Mod. Phys. **56**, 99 (1984).
[7] L. Laloux, A. Georges, and W. Krauth, Phys. Rev. B **50**, 3092 (1994).
[8] V. Janis and G. Czycholl, Phys. Rev. B **61**, 9875 (2000).
[9] F. Kagawa, T. Itou, K. Miyagawa, and K. Kanoda, Phys. Rev. Lett. **93**, 127001 (2004).
[10] A. C. Hewson, J. Bauer, and W. Koller, Phys. Rev. B **73**, 045117 (2006).
[11] J. Bauer and A. C. Hewson, arXiv:0705.3818.
[12] A. C. Hewson, Phys. Rev. Lett. **70**, 4007 (1993).
[13] A. C. Hewson, J. Phys.: Condens. Matter **13**, 10011 (2001).
[14] A. C. Hewson, J. Phys.: Condens. Matter **18**, 1815 (2006).
[15] W. Metzner and D. Vollhardt, Phys. Rev. Lett. **62**, 324 (1989).
[16] E. Müller-Hartmann, Z. Phys. B: Condens. Matter **74**, 507 (1989).
[17] A. Georges, G. Kotliar, W. Krauth, and M. Rozenberg, Rev. Mod. Phys. **68**, 13 (1996).
[18] J. M. Luttinger, Phys. Rev. **119**, 1153 (1960).
[19] H. R. Krishna-murthy, J. W. Wilkins, and K. G. Wilson, Phys. Rev. B **21**, 1003 (1980).
[20] A. C. Hewson, A. Oguri, and D. Meyer, Eur. Phys. J. B **40**, 177 (2004).
[21] R. Bulla, A. C. Hewson, and T. Pruschke, J. Phys.: Condens. Matter **10**, 8365 (1998).
[22] R. Peters, T. Pruschke, and F. B. Anders, Phys. Rev. B **74**, 245114 (2006).
[23] A. Weichselbaum and J. von Delft, e-print arXiv:cond-mat/0607497.
[24] F. B. Anders and A. Schiller, Phys. Rev. Lett. **95**, 196801 (2005).
[25] R. Bulla, Phys. Rev. Lett. **83**, 136 (1999).
[26] J. Bauer, A. C. Hewson, and A. Oguri, J. Magn. Magn. Mater. **310**, 1133 (2007).
[27] J. A. Hertz and D. M. Edwards, Phys. Rev. Lett. **28**, 1334 (1972).
[28] J. Spałek and P. Gopalan, Phys. Rev. Lett. **64**, 2823 (1990).
[29] P. S. Riseborough, Philos. Mag. **86**, 2581 (2006).
[30] R. Zitzler, T. Pruschke, and R. Bulla, Eur. Phys. J. B **27**, 473 (2002).
[31] S. V. Dordevic, K. S. D. Beach, N. Takeda, Y. J. Wang, M. B. Maple, and D. N. Basov, Phys. Rev. Lett. **96**, 017403 (2006).
[32] D. Meyer and W. Nolting, Phys. Rev. B **64**, 052402 (2001).
[33] T. Saso and M. Itoh, Phys. Rev. B **53**, 6877 (1996).
[34] Y. Ono, J. Phys. Soc. Jpn. **67**, 2197 (1998).
[35] D. Edwards and A. C. M. Green, Z. Phys. B: Condens. Matter **103**, 243 (1997).
[36] O. Buu, A. Forbes, A. van Steenbergen, S. Wiegers, G. Remènyi, L. Puech, and P. Wolf, J. Low Temp. Phys. **110**, 311 (1998).